Original

Staron, P.; Liu, J.; Riekehr, S.; Schell, N.; Huber, N.; Kashaev, N.; Mueller, M.; Schreyer, A.:

In Situ Experiment for Laser Beam Welding of Ti Alloys Using High-Energy X-Rays

In: Materials Science Forum, Mechanical Stress Evaluation by Neutrons and Synchrotron Radiation VIII (2017) Trans Tech Publications

DOI: 10.4028/www.scientific.net/MSF.905.114

Materials Science Forum
ISSN: 1662-9752, Vol. 905, pp 114-119
doi:10.4028/www.scientific.net/MSF.905.114

Submitted: 2015-10-29
Revised: 2016-05-13
Accepted: 2017-02-12
Online: 2017-08-22

In Situ Experiment for Laser Beam Welding of Ti Alloys Using High-Energy X-Rays

P. Staron[1,a*], J. Liu[1,b], S. Riekehr[1,c], N. Schell[1,d], N. Huber[1,e], N. Kashaev[1,f], M. Müller[1,g], A. Schreyer[1,h]

[1]Institute of Materials Science, Helmholtz-Zentrum Geesthacht, Max Planck-Str. 1, 21502 Geesthacht, Germany

[a]peter.staron@hzg.de, [b]liujie_go2008@hotmail.com, [c]stefan.riekehr@hzg.de, [d]norbert.schell@hzg.de, [e]norbert.huber@hzg.de, [f]nikolai.kashaev@hzg.de, [g]martin.mueller@hzg.de, [h]andreas.schreyer@hzg.de

Keywords: laser welding; high-energy X-rays; diffraction.

Abstract. The laser beam welding (LBW) process has many advantages for industrial production; however, it still has to be optimized for two-phase Ti alloys. Phase transformations and residual stresses play a crucial role for welding these alloys. Specific questions about the development of phase content during fast heating with a laser and rapid cooling can only be addressed with time-resolved in-situ experiments, avoiding artefacts from quenching. Also the residual stress development during cooling depends on the occurring phase transformations. Thus, an LBW chamber employing a fibre laser was developed for use with high-energy X-rays from a synchrotron source. Bead-on-plate welding experiments with 2.5 mm thick samples were carried out at the HZG high-energy materials science beamline (HEMS) at DESY, Hamburg. The first experiments focused on the solid-solid phase transformations in a Ti-6Al-4V alloy. Moreover, residual stresses developing during cooling were studied.

Introduction

Ti-based alloys are attractive for several applications, e.g. in aerospace industries, because of their low density and high specific strength [**1**]. A widely used alloy is the two-phase (α+β) alloy Ti-6Al-4V. Microstructure and properties of the material depend on the heat treatment it has undergone. One source of heat is welding, which is necessary to join sheets. Laser welding can be used as a fast technique with localized low heat input to join sheets of this alloy. Because of the high heating and cooling rates of the laser welding process, the material can be in a metastable state of varying phase content in the weld region. Phase analysis is required to study the microstructure after welding.

The question, however, how the resulting microstructures evolved, can only be studied in in-situ experiments. Such experiments can improve the understanding of the phase transformation kinetics and the build-up of residual stresses during laser welding. Therefore, a sample environment for in-situ laser welding experiments was built. It had also been used for studying laser welding of TiAl alloys [**2**].

Experimental Details

Synchrotron experiment. The in-situ experiments were performed at the HZG beamline HEMS (P07B) at the synchrotron source PETRA III at Deutsches Elektronen-Synchrotron (DESY), Hamburg [**3, 4**]. An incident beam with a photon energy of 87.1 keV (wavelength 0.1423 Å) from a single Si monochromator and a cross-section of 0.5 × 0.5 mm^2 was used. The X-ray and laser beams were adjusted to the same position in the middle of the plate (Fig. 1). A PerkinElmer area detector with a pixel size of 200 μm was used with a frame rate of 5 Hz. The available intensity at the main beam (P07A) currently allows frame rates that are about one order of magnitude higher than used for this work; after the planned installation of a new undulator, the available intensity will even be higher. In the future, a new PILATUS3 X CdTe area detector from DECTRIS will be available for such experiments, allowing frame rates up to 250 Hz.

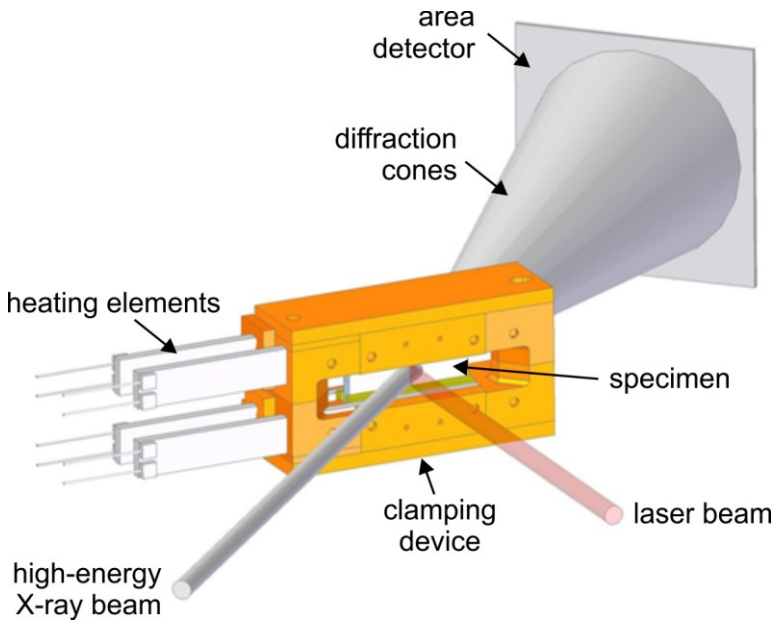

Fig. 1: Sketch of the set-up of the in-situ laser welding experiment.

Fig. 2: Sample welded in an in-situ experiment (size: 25 mm × 50 mm).

The Debye-Scherrer rings recorded with the area detector were azimuthally averaged to obtain diffraction patterns as a function of the scattering vector q for the phase analysis. For strain analyses, four sectors with a size of 20° were averaged at 0°, 90°, 180° and 270° on the rings. The 0° and 180° sectors were averaged to yield the strain in vertical direction while the 90° and 270° give the strain in horizontal direction. The vertical direction corresponds to the transverse sample direction. Since the samples are mounted under 45° to the X-ray beam (cf. Fig. 1), the horizontal direction corresponds to a direction at 45° between longitudinal and normal direction. Moreover, all results are averaged not only over the sample thickness, but also over a range of about 3.5 mm in longitudinal direction due to the 45° angle of the sample with respect to the X-ray beam. Since temperature, phase content and residual stresses can have gradients over the sample thickness as well as with the distance from the laser heat source, a corresponding averaging is present in the results obtained with this set-up. To improve the configuration, the angle between laser and X-ray beams would have to be smaller. However, the laser process required perpendicular impact on the surface.

The fibre laser optics was attached to the welding chamber. Thus, by moving the chamber horizontally and vertically, the X-ray beam could be located at different locations around the welding spot. With the current set-up, the position of the X-ray beam with respect to the laser beam is fixed during welding.

The program Fit2d was used for data reduction [**5**]. A Rietveld refinement for an analysis of the phase content was done with Maud [**6**]. The Ti α-phase with the symmetry P63/mmc and lattice parameters a = 2.91 Å and c = 4.658 Å and the Ti β-phase with the symmetry I/–43m and a lattice parameter a = 3.246 Å were used for fitting; the lattice parameters and phase fractions were refined. Single peak fitting for strain analysis was done using a Gaussian peak profile and a linear background function. A least-squares algorithm together with the Levenberg-Marquardt minimizing method were used for single peak fitting.

Material. The studied material was a standard Ti-6Al-4V alloy. The size of the specimens was 25 mm × 50 mm with a thickness of 2.5 mm. The weld line was 25 mm long. An example of the welds produced in the in-situ welding chamber is shown in Fig. 2.

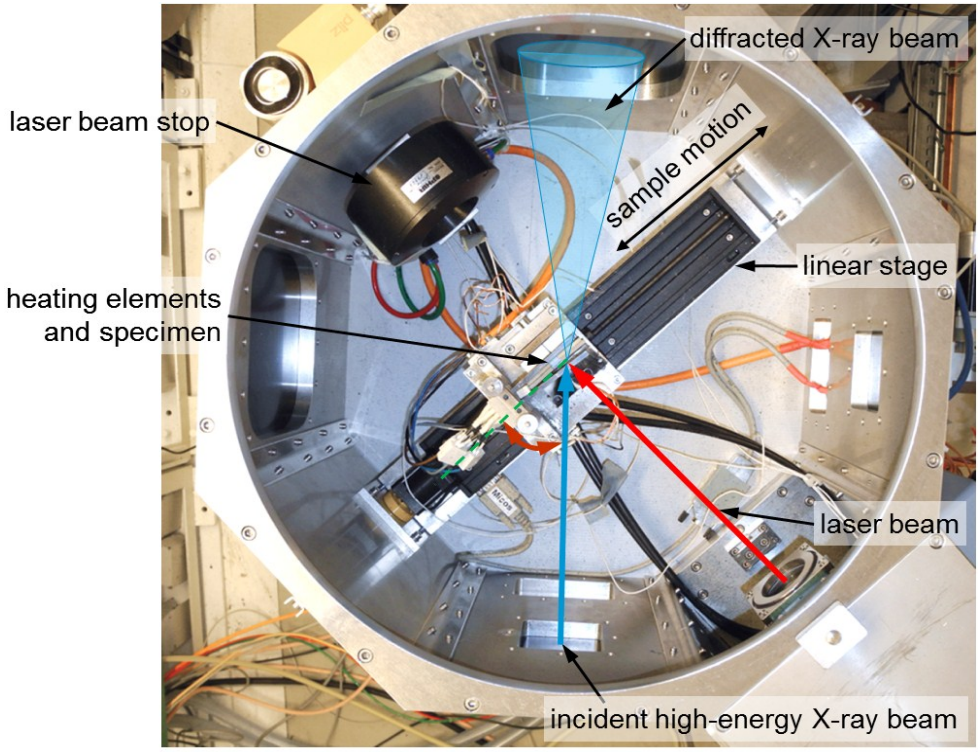

Fig. 3: Welding chamber for the in-situ experiments, top view. The chamber is closed and filled with shielding gas during welding.

Laser welding chamber. The specimens were mounted in a welding chamber filled with Ar shielding gas (Fig. 3). The chamber had Kapton windows for the incoming and diffracted X-rays. An Ytterbium fibre laser from IPG Photonics with a wavelength of 1070 nm was used for the in-situ welding experiments. The maximum laser power was 8 kW while the power used for the described experiments was 2 kW. The fibre optics was inside the welding chamber. The laser beam was aligned perpendicular to the specimen surface while the X-ray beam hits the sample at an angle of 45°. The sample could be heated to 900 °C with four ceramic resistance heaters, which was used for welding Ti-Al alloys [**2**]. In the current experiment, the heaters were only used for clamping; welding was performed at room temperature. The heating device with the sample was mounted was on a linear stage enabling sample feed during the welding action. With one single linear stage under the sample, the position of the laser beam in the sample was fixed relative to the position of the X-ray beam. This means that quasi-stationary measurements could be done with this set-up. The whole chamber was on an x-y-z stage for precise adjustment with respect to the X-ray beam.

Results

Phase transformations in the heat-affected zone. Diffraction data were taken during welding with a feed rate of 5 mm/s at various locations around the welding spot. In the following, we will report results for a location 4 mm from the weld line (lateral distance) and 2 mm behind the weld spot (longitudinal distance). At this location, transitions from the α-phase to the β-phase and back to α-phase were observed during welding (Fig. 4). The phase content in the starting material was about 93% α-phase and 7% β-phase (Fig. 5). The laser beam is turned on after 3.4 s and welding the 25 mm long sample at 5 mm/s takes 5 s; thus, the laser is switched off at 8.4 s. From 3.4 s to 6.2 s, the β phase content increases rapidly from 7% to 56% while the material heats up. From 6.2 s to 8.2 s, the phase content of α and β remain constant, indicating the heat input and dissipation was in equilibrium and the welding process was stable. When the laser beam reaches the end of the sample, no more heat can be conducted in that direction. The resulting heat concentration and temperature increase leads to the quick transformation of the remaining α into β, until after 8.7 s all α has transformed to β. Upon cooling, β transforms back to α; after 16 s, about 90% α is present.

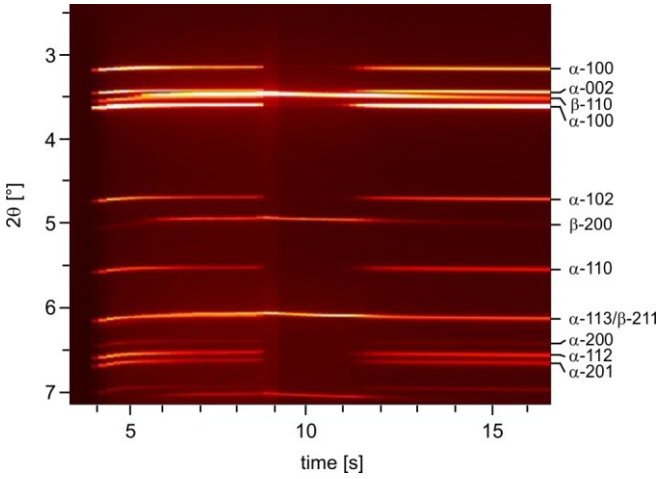

Fig. 4: Colour-coded intensity of diffraction patterns as a function of time. One pattern was taken every 200 ms.

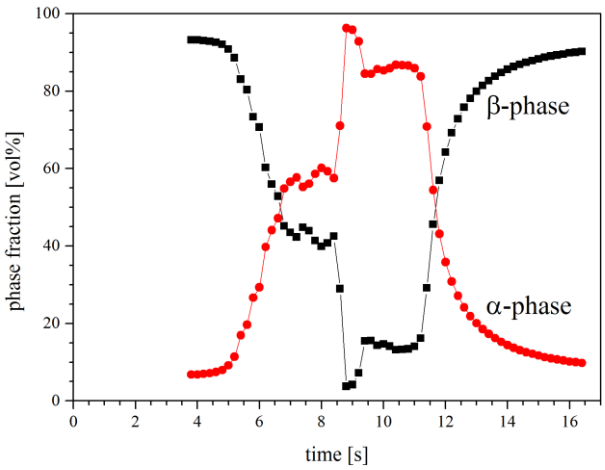

Fig. 5: Phase fractions as a function of time as obtained from full-pattern fitting with Maud.

Residual stresses. The fatigue properties of a weld are strongly influenced by the residual stress state of the material. Thus, the knowledge about welding-induced residual stresses is essential. The in-situ experiment enables studying the development of residual stresses during cooling and phase transformations. In this case, data taken from the same location as discussed above were analysed. The lattice parameters of the α-(102) and β-(211) lattice planes reflect the fast heating at the beginning of the process and the slower cooling at the end of the process (Fig. 6). During cooling, the lattice parameters in the two directions parallel (longitudinal) and perpendicular (transverse) to the welding line evolve differently, indicating the build-up of deviatoric residual stress.

Residual stresses in three orthogonal directions x, y, z (or longitudinal, transverse, normal) can be calculated from the strains using:

$$\sigma_i = \frac{E(1-\nu)}{(1+\nu)(1-2\nu)}\varepsilon_i + \frac{E(1-\nu)}{(1+\nu)(1-2\nu)}(\varepsilon_x + \varepsilon_y + \varepsilon_z) \tag{1}$$

where $i = x, y, z$ and E, ν, are diffraction elastic constants. The difference between stresses in two directions reduces to:

$$\sigma_i - \sigma_j = \frac{E(1-\nu)}{(1+\nu)(1-2\nu)}(\varepsilon_i - \varepsilon_j) = \frac{E(1-\nu)}{(1+\nu)(1-2\nu)}\frac{d_i - d_j}{d_0} \tag{2}$$

Since the stress-free lattice parameter d_0 appears only in the denominator in equation 2, an approximation can be used for d_0 and the resulting error is of second order and can be neglected. Fig. 7 shows the difference in residual stress between the transverse direction (vertical) and the projection of stresses at 45° to the longitudinal direction (horizontal), which can be calculated from the difference in the lattice parameters (Fig. 6). The diffraction elastic constants used for the calculation were: E = 117 GPa, ν = 0.315 for the α-102 reflection and E = 111 GPa, ν = 0.329 for the β-211 reflection. Two different stages can be distinguished, in which the residual stress difference increases linearly with time: The first one lasts up to 21 s and correlates with an increase of the α-102 peak width, which indicates plastic deformation (Fig. 8). It is not expected that stress gradients over the sample thickness contribute significantly to the increase in peak width because in that case the same effect should be observed for the β-phase, which is not the case (Fig. 8b). The peak width increases step-like in both phases when cooling sets in and α-phase starts to form (Fig. 8). In the second stage, the slope of the stress difference is smaller and the peak width is almost constant. The stress difference in both phases has the same magnitude.

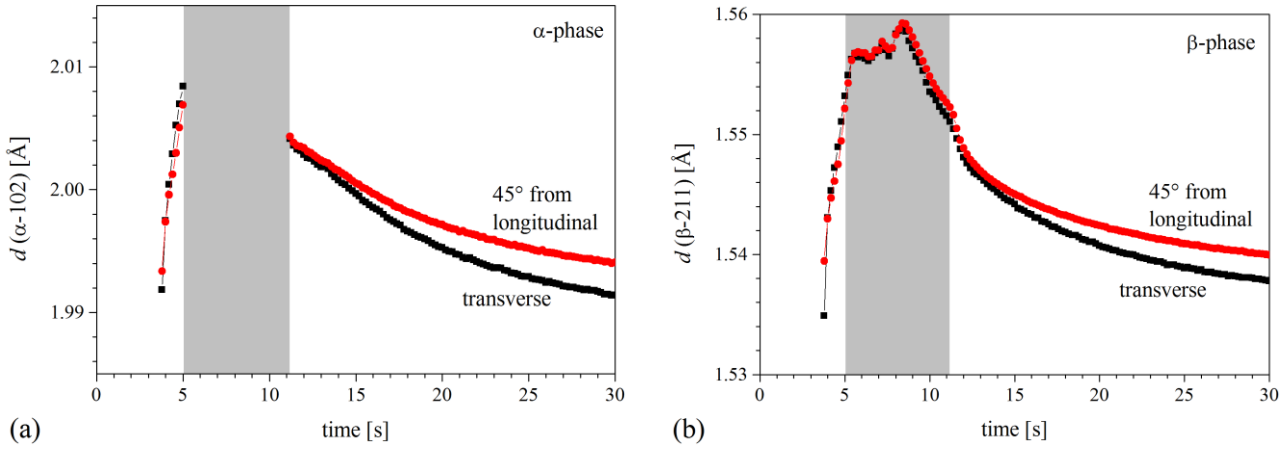

Fig. 6: Lattice parameters of the α-(102) (a) and β-211(b) reflections as a function of time. The transverse direction is perpendicular to the weld line, the second direction is at 45° between longitudinal (parallel to the weld line) and normal directions.

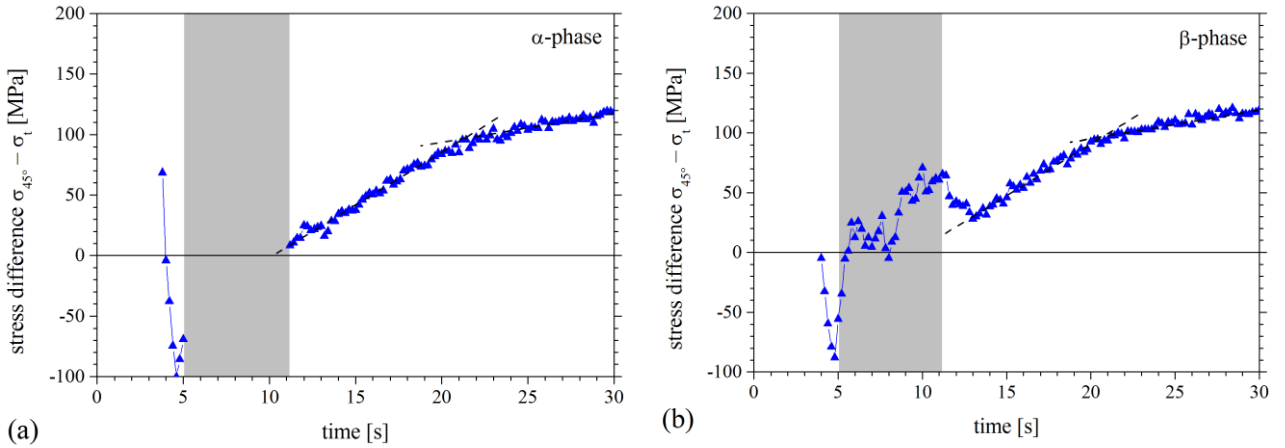

Fig. 7: Residual stress difference ($\sigma_{45°} - \sigma_{trans}$) as a function of time, calculated from the α-102 (a) and β-211 (b) reflections.

The stress difference, however, contains limited information and absolute values should be obtained in further in-situ experiments.

Summary and Outlook

The laser welding process of Ti-6Al-4V alloy was studied in an in-situ experiment using high-energy X-rays. The first results show that phase transformations in the heat-affected zone as well as residual stress formation in the weld can be monitored in the 2.5 mm thick samples with a time resolution of 200 ms. The difference in residual macro stresses in the transverse direction and the direction 45° from the longitudinal direction was 120 MPa after 30 s.

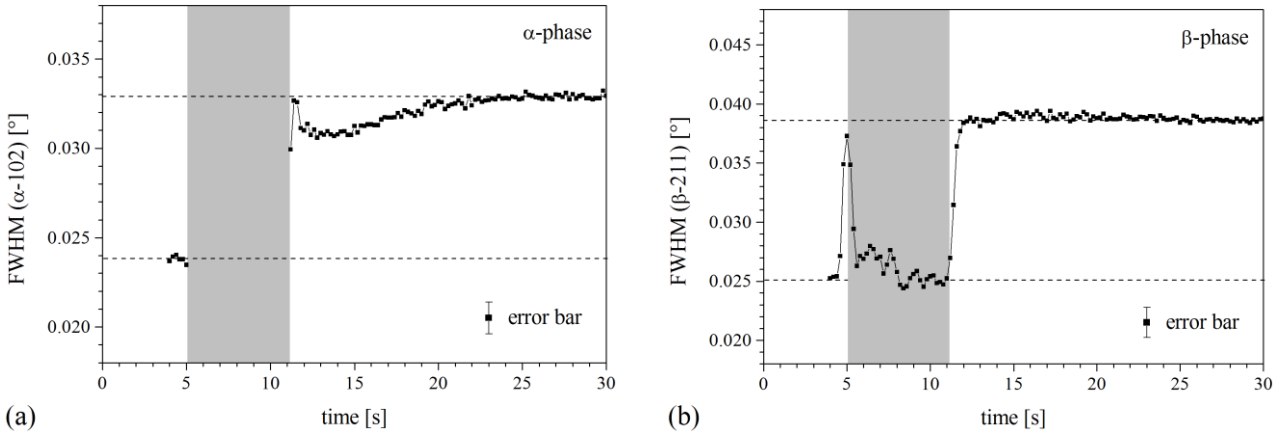

Fig. 8: Peak widths (full width at half maximum, FWHM) as a function of time for the α-102 and β-211 reflections.

With measurements performed at different incident X-ray angles, it could be possible to extrapolate to the longitudinal stress direction in order to fully describe the residual stress state during the welding process. With faster high-energy X-ray area detectors the time resolution can be increased to be able to better resolve the fast heating by the laser and the initial cooling stages. Moreover, with an additional movement of the laser optics, transient measurements of the process will become possible where the history of a fixed sample volume can be followed. This, however, requires a larger and more complex welding chamber with an additional linear axis.

Acknowledgements

The authors acknowledge the excellent technical support of René Kirchhoff in the design and construction of the welding chamber and the support during the experiments. The technical support of René Dinse, Gerhard Kocik and Bernhard Eltzschig are gratefully acknowledged.

References

[1] C. Leyens, M. Peters (eds.). Titanium and Titanium Alloys: Fundamentals and Applications. Wiley-VCH, Weinheim (2003).

[2] J. Liu, P. Staron, S. Riekehr, A. Stark, N. Schell, N. Huber, A. Schreyer, M. Müller, N. Kashaev, In situ study of phase transformations during laser-beam welding of a TiAl alloy for grain refinement and mechanical property optimization, Intermetallics 62 (2015) 27–35.

[3] P. Staron, N. Schell, A. Haibel, F. Beckmann, T. Lippmann, L. Lottermoser, J. Herzen, T. Fischer, M. Koçak, A. Schreyer. The New GKSS Materials Science Beamlines at DESY: Recent Results and Future Options. Mater. Sci. Forum 638–642 (2010) 2470–2475.

[4] N. Schell, A. King, F. Beckmann, T. Fischer, M. Müller, A. Schreyer, The High Energy Materials Science Beamline (HEMS) at PETRA III, Mater. Sci. Forum 772 (2014) 57–61.

[5] A.P. Hammersley. FIT2D: An Introduction and Overview. ESRF Internal Report (1997) ESRF97HA02 T.

[6] H.R. Wenk, L. Lutterotti, S.C. Vogel. Powder Diffr. 25 (2010) 283–96.